



Trans. Nonferrous Met. Soc. China 30(2020) 1560-1573

Transactions of Nonferrous Metals Society of China

www.tnmsc.cn



Hot working behavior of near alpha titanium alloy analyzed by mechanical testing and processing map

Maryam MORAKABATI, Alireza HAJARI

Faculty of Material & Manufacturing Technologies, Malek-Ashtar University of Technology, Shabanlou Street, Tehran, Iran

Received 4 September 2019; accepted 14 April 2020

Abstract: The hot deformation characteristics of the Ti–5.7Al–2.1Sn–3.9Zr–2Mo–0.1Si (Ti-6242S) alloy with an acicular starting microstructure were analyzed using processing map. The uniaxial hot compression tests were performed at temperatures ranging from 850 to 1000 °C and at strain rates of $0.001-1~\rm s^{-1}$. The developed processing map was used to determine the safe and unsafe deformation conditions of the alloy in association with the microstructural evolution by SEM and OM. It was recognized that the flow stress revealed differences in flow softening behavior by deformation at 1000 °C compared to the lower deformation temperatures, which was attributed to microstructural changes. The processing map developed for typical strain of 0.7 in two-phase field exhibited high efficiency value of power dissipation of about 55% at 950 °C and $0.001~\rm s^{-1}$, basically due to extensive globularization. An increase in strain rate and a decrease in temperature resulted in a decrease in globularization of α lamellae, while α lamellar kinking increased. Eventually, the instability domain of flow behavior was identified in the temperature range of 850–900 °C and at the strain rate higher than $0.01~\rm s^{-1}$ reflecting the flow localization and adiabatic shear banding. By considering the power efficiency domains and the microstructural observations, the deformation in the temperature range of 950–1000 °C and strain rate range of $0.001-0.01~\rm s^{-1}$ was desirable leading to high efficiencies. It was realized that (950 °C, $0.001~\rm s^{-1}$) was the optimum deformation condition for the alloy.

Key words: Ti-6242S; hot deformation; processing map; microstructure; globularization

1 Introduction

Near- α titanium alloys are extensively used in jet engines as compressor discs and blades due to their high specific strength, corrosion resistance, superior fatigue and creep properties at elevated temperatures [1]. A series of hot working and heat treatment steps are usually performed on melted ingot to prepare titanium mill products [2,3]. In the first step, the preliminary hot working/annealing is conducted in the single-phase β field to break the cast structure and to produce a uniformly wrought microstructure. Depending on the cooling rate from the β field, the morphology of the transformed microstructure might be lamellar widmanstätten (basketweave), or fine acicular [4]. After β working/annealing operations, transformed microstructure is broken down and dynamic globularization of α phase occurs by secondary hot deformation in the $\alpha+\beta$ phase field. Finally, heat treatment is conducted in the $\alpha+\beta$ phase region in order to control the microstructural parameters such as volume fraction and morphology of α phase and to achieve a combination of good mechanical properties [5,6]. The second step of thermomechanical processing plays a key role in developing an equiaxed microstructure frequently desired for final shaping or in service. Previous researches have indicated that in addition to the processing parameters (i.e., temperature, strain rate and strain), initial microstructure has also a major effect on the behavior of the near- α titanium alloys during secondary hot deformation [7]. For instance,

Corresponding author: Maryam MORAKABATI; Tel: +98-21-22936494; E-mail: m_morakabati@mut.ac.ir DOI: 10.1016/S1003-6326(20)65319-5

SEMIATIN and BIELER [4] concluded that the strain rate sensitivity value of the Ti-6Al-4V alloy with the acicular initial microstructure is greater than the lamellar microstructure with thick α -lamellae. This causes different restoration phenomena during hot deformation. LI et al [8] investigated the effect of initial α lamellar thickness on the deformation behavior of Ti-5.4Al-3.7Sn-3.3Zr-0.5Mo-0.4Si alloy. They showed that the value of apparent activation energy increases with decreasing initial α platelet thickness. The acicular initial microstructure is more easily fragmented and dynamically globularized into fine α phase, while thick initial lamellar microstructure undergoes buckling and elongates. Similar results were also reported by SEMIATIN et al [9] for Ti-6Al-4V alloy. Furthermore, LÜTJERING and WILLIAMS [3] reported that the microstructure after the primary deformation in the β region contains β grains with various sizes surrounded by the α phase boundaries. Moreover, the lamellar α phase will be formed in the β grains during cooling. In a previous investigation [10], it has been found that the presence of α -grain boundary resulted from inhomogeneous slow cooling causes an deformation.

Among all titanium alloys, Ti-6242S alloy is one of the developed near- α Ti alloys, exhibiting good combination of mechanical properties in high-temperature services (~550 °C) [11]. Studies conducted on the Ti-6242S alloy were started from duplex (bimodal) and thick lamellar α initial microstructure [12,13]. Due to the importance of initial microstructure and thickness of α lamellae on the secondary hot deformation behavior and microstructural evolutions, investigation on the hot deformation behavior of the Ti-6242S with acicular initial microstructure is really important. Therefore, in the current research, an initial acicular microstructure after recrystallization annealing in β phase region followed by quenching in water was selected as starting microstructure. Here, the main goal is to investigate the flow behavior and microstructural transformation of the Ti-6242S alloy with an acicular initial microstructure during secondary hot deformation. Furthermore, processing map was developed to determine the appropriate range of deformation of the alloy.

2 Experimental

A Ti-5.7Al-2.1Sn-3.9Zr-2Mo-0.1Si (wt.%) ingot was manufactured through double melting in a vacuum arc remelting furnace. To remove casting structure and reduce the segregation, the ingot was homogenized for 5 h at 1150 °C and then primarily hot-rolled at the same temperature to a reduction of 70%. As depicted in Fig. 1(a), the microstructure of the as-received strip consisted of the transformed β structure surrounded by α grain boundaries. The transformed β phase contained the secondary α lamellae phase with thin layer of β phase retained between it. The prior β grain size was estimated to be about (280±8) µm by quantitative measurement. The β transus temperature (temperature at which $\alpha + \beta \leftrightarrow \beta$) was measured by metallographic method to be around 1010 °C. The as-received Ti-6242S was treated via solution treatment at 1050 °C for 35 min followed by quenching in water to obtain an acicular microstructure. The optical micrograph of the heat-treated sample is shown in Fig. 1(b). The acicular microstructure contained fine martensitic α phases (α') distributing in the large β grains. The average grain size of the initial microstructure was determined to be (405±5) µm. The volume fractions of α' and β phases were estimated to be 2.1% and 97.9%, respectively. The cylindrical hot compression test specimens taken from heat-treated material were machined with their perpendicular to rolling direction to 13.33 mm in diameter and 20 mm in length (in accordance to ASTM E209, preserving the aspect ratio). Uniaxial compression tests were performed by an Instron 8502 testing machine coupled with resistance furnace. A thin layer of graphite was put as a lubricant to minimize the friction between the anvils and specimens. To investigate the effect of deformation on the microstructure evolution of the alloy, it is necessary to study the prior hot deformation microstructure. Four cylindrical specimens were pre-heated at testing temperatures of 850, 900, 950 and 1000 °C for 5 min and quenched in water. Another four cylindrical specimens held at the mentioned test temperatures for 5 min deformed under the initial strain rates of 0.001, 0.01, 0.1 and 1 s^{-1} up to the true strain of 0.7

followed by water quenching. For microstructural investigations, sections of deformed specimens were cut parallel to compression axis and prepared by standard metallographic techniques. specimens were mechanically polished by alumina and etched with a solution of 1 mL HF + 2 mL $HNO_3 + 97 \text{ mL } H_2O$ for 15-30 s. The microstructural observation was carried out on an Olympus BX51 optical microscope (OM) and a Tescan VEGA3 scanning electron microscope (SEM). CLEMEX image analysis software as a quantitative metallurgy tool was employed to analyze the microstructural features. The average grain size and volume fraction of the phases were measured according to ASTM E-112 and ASTM E-562, respectively.

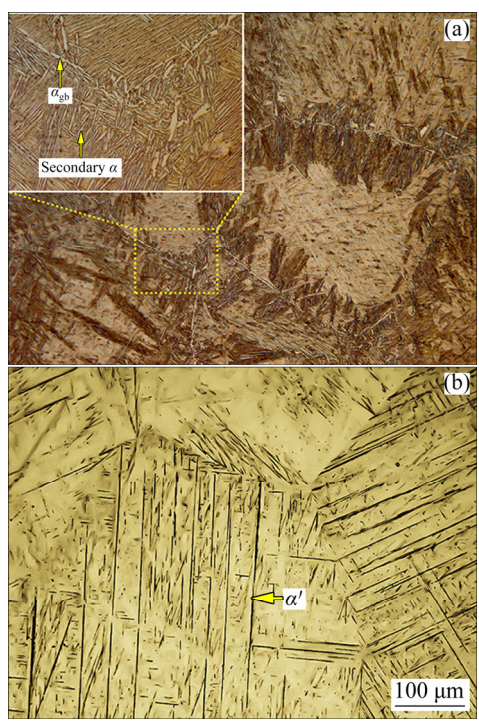


Fig. 1 Microstructures of as-received (a) and heat-treated Ti-6242S rolled strip at 1050 °C for 35 min followed by water quenching (b)

3 Results and discussion

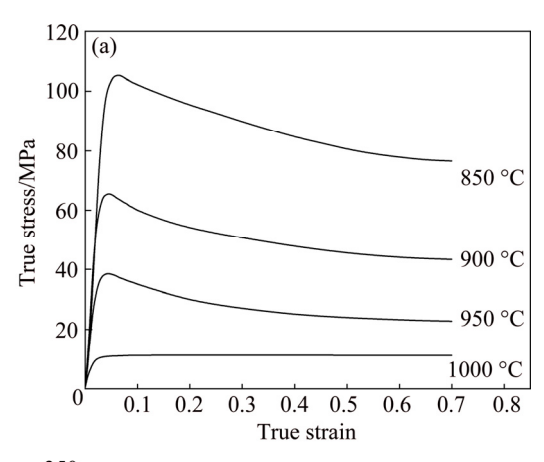
3.1 Stress-strain curve

3.1.1 General behavior

As reported in previous work [14], despite the use of lubricant, the effect of specimen/anvil interface friction on flow stress is non-negligible. Moreover, deformation heating due to the low thermal conductivity relative to other metals has a significant effect on flow stress during hot

deformation. Hence, the flow behavior of the alloy was analyzed via stress—strain curves corrected for friction and deformation heating effects following the method by EVANS and SCHARNING [15] and DIETER et al [16], respectively.

Figure 2 shows the stress-strain curves for the acicular starting microstructure deformed in the temperature range of 850-1000 °C and the strain rates of 0.001 and 0.1 s⁻¹, respectively. As shown, the flow stress exhibits an increase with strain until peak stress due to the production and interaction of dislocations in initial stage of deformation [17]. In addition, the different behaviors can be seen in the softening response of the flow curves by deformation in the lower part of α/β region $(T \le 950 \,^{\circ}\text{C})$ compared to its upper part $(T = 1000 \,^{\circ}\text{C})$. At 1000 °C, at strains greater than the peak strain, the flow curves reached to steady-state condition. This behavior is due to an increase in the volume fraction of β -BCC phase with high stacking fault energy and diffusivity compared to the α -HCP phase at 1000 °C against lower temperatures [18]. Similarly, REZAEE et al [19] also observed that the



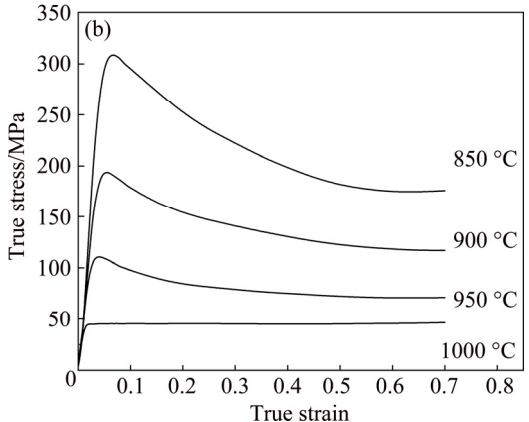


Fig. 2 Typical true stress–true strain curves of deformed specimens in temperature range of 850-1000 °C and under strain rates of 0.001 (a) and 0.1 s^{-1} (b)

flow softening behavior in the upper part of α/β region is significantly different compared to its lower part. As illustrated in Fig. 2, beyond the peak stress, the curves dropped and steady state condition was observed at strain value larger than about 0.6 at or below deformation temperature of 950 °C. This behavior indicated that dynamic softening counteracts the work-hardening of the material during the compression.

As seen in Fig. 2, the flow stress decreased with increasing the deformation temperature at a constant strain rate. In this case, the influence of thermally-activated processes and an increase in the kinetic energy of atoms reduces the critical shear stress for slip. Increasing the volume fraction of β phase with more active slip system than α phase, is another effective factor on this behavior [19]. On the other hand, flow stress increased with increasing the strain rate. The main reason for this phenomenon is the fewer opportunities provided to reduce energy level by an increase in strain rate.

Different reasons have been reported in the literature, which may be hypothesized as causes for the observed flow softening. JIA et al [20] believe that break-up and globularization of lamellar α phase at lower strain rates and adiabatic shear banding at higher strain rates can be the reasons of flow softening in two-phase titanium alloys during hot deformation below β -transus temperature. Another theory for explanation of flow softening in titanium alloys is the platelet bending/buckling [21]. In addition, as the critical strain needed for globularization initiation is much higher than that of flow softening initiation [22], other mechanisms may also contribute to flow softening including crystallographic texture formation during deformation. Another studies indicated that the rotation of colonies and α lamellae toward softer orientations with low Taylor factor and slip transmission across the α/β interfaces are the main reasons for flow softening in two-phase titanium alloys with lamellar structure [23]. In the present work, adiabatic shear banding and globularization of lamellar α phase are the main mechanisms showing flow softening.

3.1.2 Effect of temperature on steady-state stress

The steady-state stresses as a function of deformation temperature at various strain rates are shown in Fig. 3. It can be seen that, at a constant strain rate, the flow stress decreased continuously

with increasing deformation temperature. It is clear that the dependency of the steady-state stress on the deformation temperature decreases with an increase in the deformation temperature. The temperature dependence of the flow stress at different temperatures can be attributed to two phenomena: (1) Simultaneous deformation of α and β phase shows high sensitivity at low temperatures where the diffusion is slow and low sensitivity at high temperatures where rapid diffusion occurs [24]. In words, increasing other the deformation temperature increases the volume fraction of β phase with higher diffusivity compared to α phase and consequently, decreases the temperature dependency of the flow curve. (2) The $\beta \rightarrow \alpha + \beta$ phase transformation occurs and the dominant affects deformation mechanism phase characteristics. In near- α titanium alloys, due to high kinetics of β to α transformation [25], the volume fraction of α phase increases rapidly with decreasing temperature at temperature below β -transus temperature. Therefore, as α phase has higher strength and lower active slip system than β phase [26], the flow stress increases by a decrease in deformation temperature. This behavior has also been reported for IMI834 alloy [24].

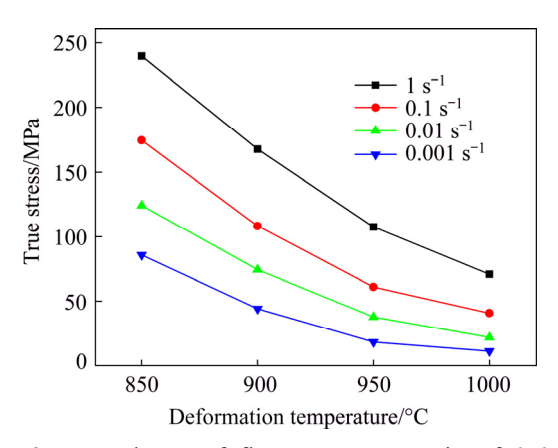


Fig. 3 Dependency of flow stress at strain of 0.6 on deformation temperature for various strain rates

3.2 Microstructural features associated with deformation

3.2.1 Microstructures prior to deformation

To investigate the effect of deformation on the evolution of microstructure in the Ti-6242S alloy, it is necessary to study the prior hot deformation microstructure. The microstructural changes during pre-heat treatment for temperatures of 850, 900, 950 and 1000 °C are shown in Fig. 4. As expected,

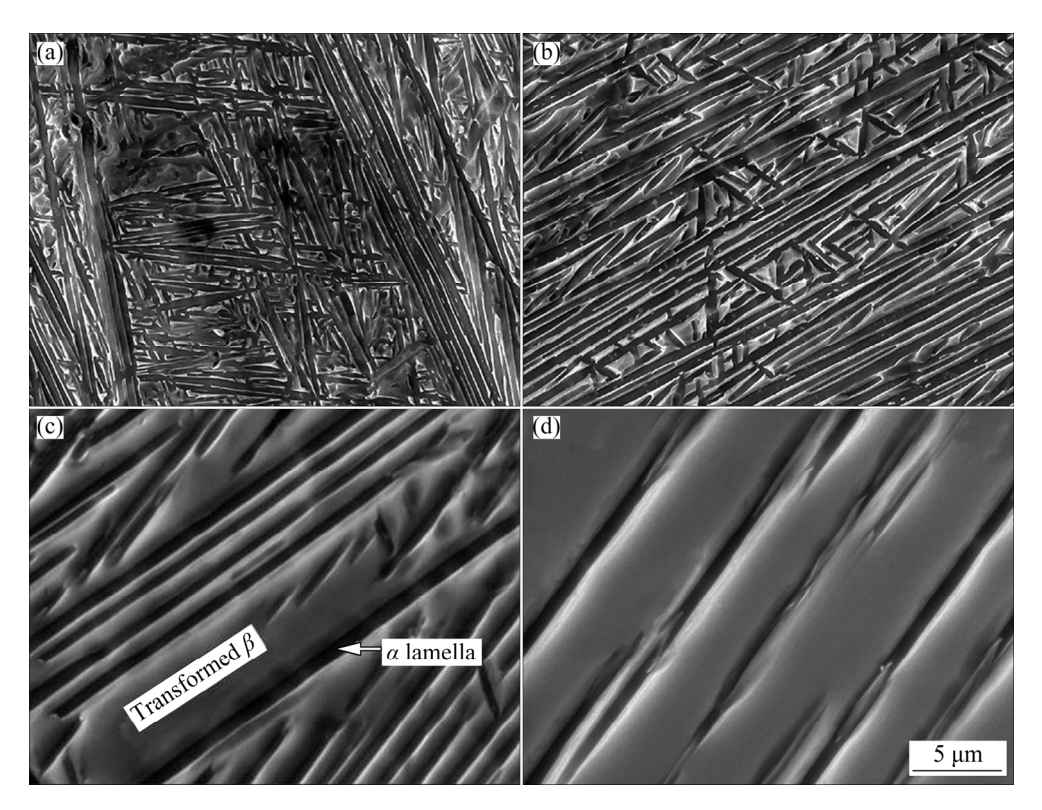


Fig. 4 Microstructures of water-quenched specimens after soaking at 850 (a), 900 (b), 950 (c) and 1000 °C (d) prior to deformation

the initial martensitic microstructure transformed to thin lamellar microstructure during the prior deformation pre-heat treatment. The microstructural examinations showed that thickness of α lamellae varied to 0.23 and 0.61 μ m at 850 and 1000 °C, respectively.

The variations of the volume fraction of β phase versus the pre-heat temperature are shown in Fig. 5. It is clearly observed that the temperature of prior deformation has a significant effect on the volume fraction of α and β phases. As seen, the volume fraction of β phase was determined to be 23.1%, 36.5%, 72.4% and 84.3% at pre-heat treatment temperatures of 850, 900, 950 and 1000 °C, respectively. Microstructural evolution has also been reported recently for IMI834 near-α titanium alloy [24]. By comparing Fig. 5 with Fig. 3, the dependence of flow stress on the volume fraction of α and β phases at different temperatures is clearly observed. As seen, the flow stress decreased with increasing the volume fraction of β phase, which is due to the lower strength of β phase compared to α phase.

3.2.2 Effect of deformation temperature

As seen in Fig. 2, the flow curves exhibited a

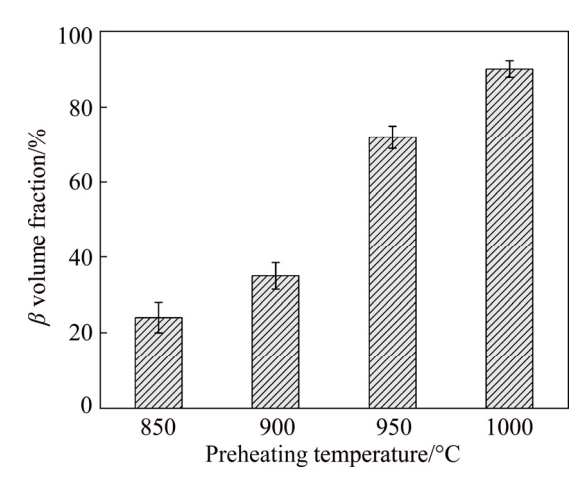


Fig. 5 Volume fraction of β phase at different preheating temperatures

peak flow stress at relatively low strains followed by flow softening. Such behavior in single-phase alloys is often attributed to occurrence of DRX, i.e., the nucleation and growth of new grains. However, different microstructural evolutions are known to be responsible for the observed flow softening in two-phase Ti alloys [27].

The effect of temperature on the microstructure of the Ti-6242S alloy deformed at a

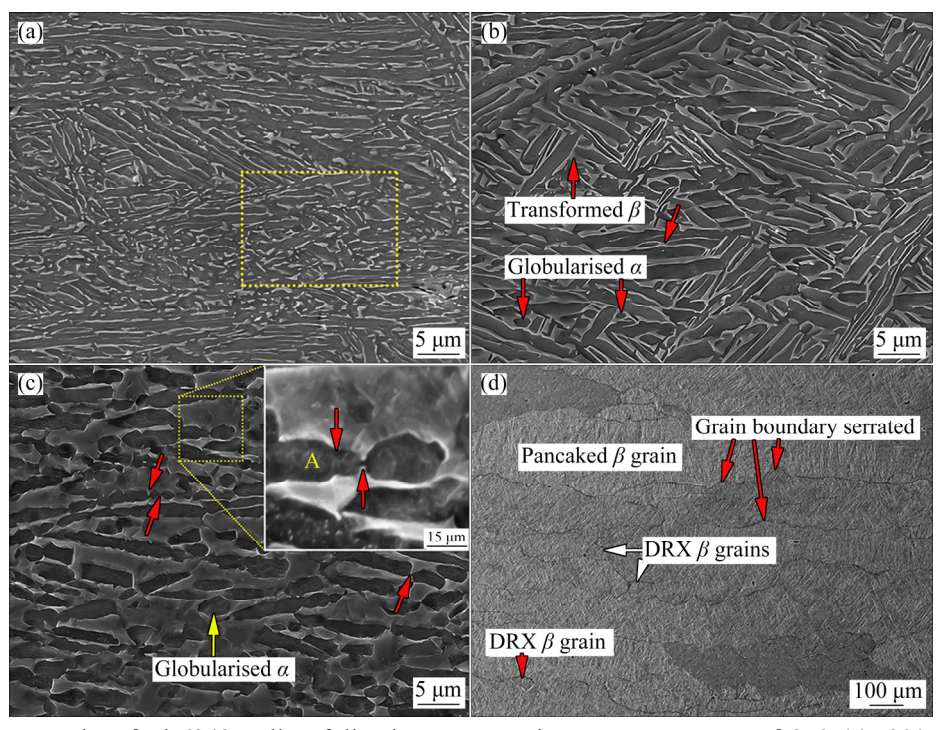


Fig. 6 SEM micrographs of Ti-6242S alloy following compression at temperatures of 850 (a), 900 (b), 950 (c) and 1000 °C (d) under strain rate of 0.01 s⁻¹

strain rate of 0.01 s⁻¹ is presented in Fig. 6. As seen, the deformation temperature played an important role in the microstructural characteristics. According to Fig. 6, the evolution of α lamellar phase, during dynamic globularization and kinking, was a prevailing microstructure feature at deformation temperatures of 950 °C or lower; while at 1000 °C, the dynamic recovery and partial recrystallization of β phase was dominant, mainly due to an increase in β volume fraction, with BCC structure. Therefore, the microstructural developments during deformation temperature range of 850-1000 °C can be divided into two parts. Generally, the main characteristics of microstructural evolution during deformation at 850–950 °C is the rotation of α colonies to be perpendicular to the compressive axis, platelet bending/buckling, kinking as well as globularization of α phase. As seen in Fig. 6, the degree of dynamic globularization of α -lamellae increased with an increase in the temperature, while the lamellae became coarser and their aspect ratio decreased. Indeed, by increasing the temperature, interfaces migration is facilitated due to powerful diffusional effect accelerating the globularization process of lamellae and accordingly increasing the globularized fraction. The similar findings have been reported previously for globularization of

Ti600 alloy [28].

Earlier researches proposed two main mechanisms to reach the globularized α -phase, i.e., boundary-splitting and termination migration. The first mechanism is the sub-boundary formation associated with the instability of 90° dihedral angles between interphase of α/α boundaries known as boundary-splitting. The α/α sub-boundaries may be formed across the α -lamellae either through formation of a recovered substructure or intense localized shear during hot deformation. Diffusion of β phase as an inter-lamellar phase into the boundaries makes a reduction in dihedral angle and finally results in a groove in α -lamellae. Termination migration is driven by a reduction in surface energy via mass transport from the curved surfaces of the lamellar terminations to adjacent flat surface of the lamellae and it is diffusion control [29]. As seen in Fig. 7, a comparison of the thickness of α -lamellae prior to deformation and the thickness of the α particles after deformation at a given strain rate and various temperatures also suggests that the termination migration may play a role during dynamic globularization as reported by STEFANSSON and SEMIATIN [29] for static globularization. The details of these processes are illustrated in Fig. 8, graphically.

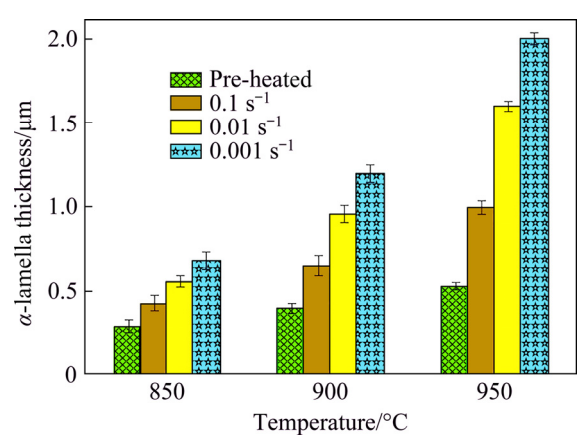


Fig. 7 Variation of α -lamella thickness with deformation temperature and strain rate

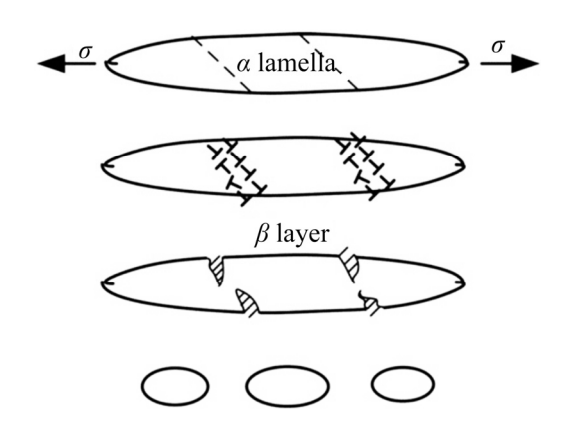


Fig. 8 Schematic diagram illustrating steps of globularization process [29]

As observed in Fig. 6, it is expected that the effect of diffusion increases by increasing the deformation temperature, due to higher diffusion rate at deformation temperature of 950 °C as compared to temperatures of 900 and 850 °C. As seen in Fig. 6(c) with white arrow, dislocation density increased in "A" layer as a sub-boundary was formed due to deformation and imposed shear strain. The formation of unstable α/α interface provided favorable conditions for penetration of β phase into groove. Hence, the fragmentation of α layer occurred and α/β interface formed. According to the nature of this diffusional process, it would be expected that the separation of two sub-grain and the formation of α/β interface can be completed by increasing the deformation time and thus the aspect ratio of α lamellae decreases. Such mechanism can be observed at deformation temperature of 900 °C (red arrow in Fig. 6(b)).

One of the differences observed in the microstructure of the alloy deformed at $850~^{\circ}\text{C}$ as

compared to higher temperatures is that, the continuity of the β phase was lost and it was fragmented to separate particles with various lengths. Earlier researches on warm working of Ti-6Al-4V [23] revealed that division of the β phase is associated with (1) local shear deformation (white arrow in Fig. 6(a)), (2) boundary splitting, and (3) local dissolution.

Figure 6(d) shows the microstructure of the specimen deformed at the near β -transus temperature at a strain rate of 0.01 s⁻¹. As seen, the microstructure of the specimen deformed at 1000 °C contained β phase and discontinuous α layers at the prior β grain boundaries and also within gains. Despite these microstructural differences, the effect of deformation at 1000 °C on microstructural evolution is similar to that in the research [19] on hot working of Ti-6242 alloy in the β phase region. Figure 9 shows the influence of effective strain on the microstructure evolution of the specimen deformed at 1000 °C and 0.01 s⁻¹ the surface, quarter depth and center. BUCKINGHAM et al [30] showed that the lowest level of strain was seen close to the surface, gradually increasing to a maximum at the compression center where levels of deformation are the greatest. As seen in Fig. 9(a), α platelets were present within the β grains as well as grain boundaries in areas close to the surface. By increasing the distance from the surface, the β grains elongated in the plane perpendicular to the compression direction and the serration of grain boundaries due to dynamic recovery became more intensified. Additionally, small amounts recrystallized grains were apparent in the vicinity of the deformed grain boundaries. It was shown in Fig. 2(a), when the deformation was performed at 1000 °C, the stress-strain curves showed the steady-state behavior after peak stress, which is typical of dynamic recovery. This is obviously due to the high stacking fault energy and high diffusivity in the β phase [8]. Therefore, the steady-state behavior is due to dynamic softening mechanism (i.e., DRX) not being sufficient to counteract the work-hardening of the material during the hot compression at this temperature. Previous research [24] has also reported that this behavior is always observed during hot working of titanium alloys at the lower strain rates and higher deformation temperatures in the two phase region.

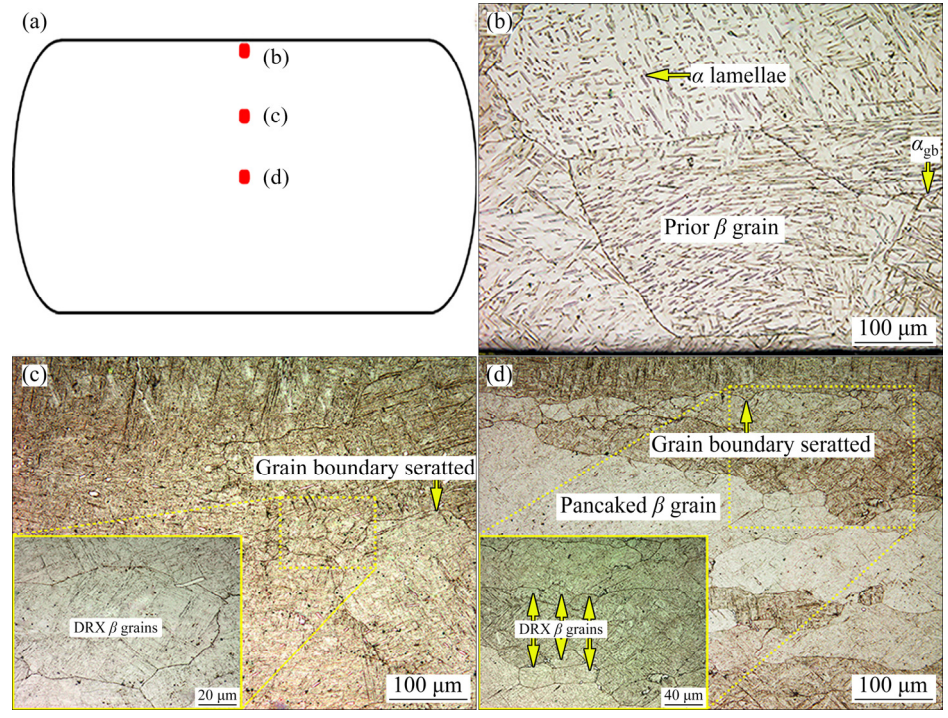


Fig. 9 Schematic picture (a) and microstructures (b–d) of Ti-6242S compressed at 1000 °C with strain rate of 0.01 s⁻¹ in different zones: (b) Surface; (c) Quarter depth; (d) Center

As seen in Fig. 9, it is clear that the volume fraction of α phase significantly decreased by comparing the microstructures at surface (Fig. 9(b)) versus those in the center (Fig. 9(d)). Adiabatic heating calculation indicated that increasing the temperature at the center of the specimen deformed at 1000 °C and strain rate of 0.01 s⁻¹ is about 2 °C. The details of deformation heating calculation had been described precisely elsewhere [30]. As the center of the compressed specimen experienced higher temperature and larger strain compared to its center part, the volume fraction of α phase decreased. This phenomenon has been also reported for different titanium alloys [31].

3.2.3 Effect of strain rate

Strain rate affects the microstructural evolution differently depending on deformation temperature. Figures 10(a, b) show the microstructures of the specimens deformed at different strain rates and 850 °C. As mentioned in Fig. 7 and clearly observed in Figs. 10(a, b), the thickness of α lamellae increased with decreasing strain rate, as the deformation time extended leading to more diffusion. This difference in α thickness suggested that the coarsening process has occurred during the deformation. It is worth noting that the coarsening process is driven by a reduction in surface energy.

When the alloy was deformed at 0.001 s⁻¹, the elongated α lamellae are arranged in parallel within α colonies. As seen in Fig. 10(b), the kinked α lamellae increased and fragmentation of the lamellar structure was apparent by increasing strain rate from 0.001 to 0.1 s⁻¹. Therefore, the aspect ratio of α lamellae decreased. In fact, dislocation accumulation rate is relatively high at higher strain rates, thus the dislocation density is accumulated rapidly to a high level and the fragmentation occurs [29]. Furthermore, SHAMS et al [2] have the reported that continuous dynamic recrystallization and emergence of new α/α grain boundary are the main restoration mechanisms at low deformation temperature in near-α Ti-1100 alloy with acicular initial microstructure.

Differently, as observed in Figs. 10(c, d), the globularization of α lamellae increased with decreasing the strain rate at deformation temperature of 950 °C. This observation is related to the fact that the globularization of α lamellae, i.e., boundary-splitting and termination migration, is a thermally-activated (diffusional) process. At this temperature, an increase in diffusion rate played fundamental roles in the penetration of β phase within the α/α sub-boundaries and globularization of α phase.

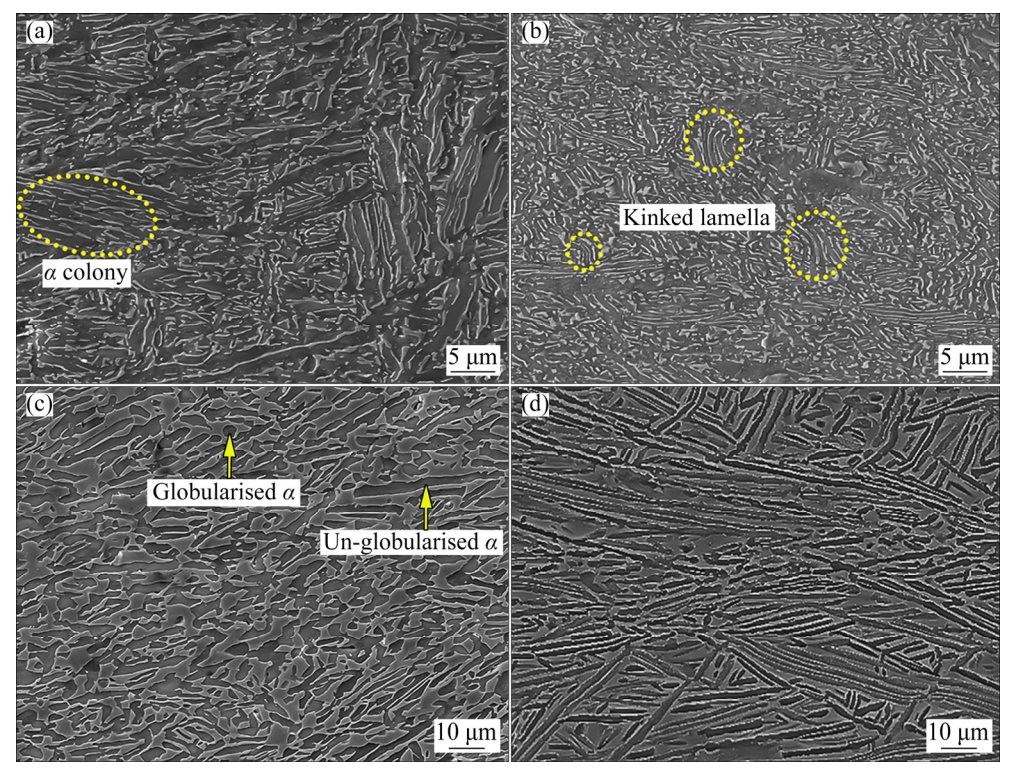


Fig. 10 SEM micrographs of Ti-6242S alloy following compression at 850 (a, b) and 950 °C (c, d) under strain rates of 0.001 (a, c) and 0.1 s⁻¹ (b, d)

The strain-rate sensitivity (m) is usually used to determine the superplastic behavior and the deformation mechanism of the material. The strain-rate sensitivity versus strain is plotted at different temperatures and strain rates, as presented in Fig. 11. As seen, the m-values increase by decreasing the strain rate and increasing the deformation temperature. This is due to changes in deformation mechanisms and easy diffusion [32]. Similar trend has been reported in the literature for this alloy with bimodal and lamellar microstructure. However, the *m*-values for the initial acicular microstructure in the present work tend to be slightly higher than those for the thick-lamellar microstructure reported by SEMIATIN LAHOTI [12] mainly due to a higher globular fraction formed from thinner α lamellae.

In Fig. 11, the maximum m-value of 0.33 was obtained at 950 °C and strain rate of 0.001 s⁻¹. As observed in Fig. 11, the strain-rate sensitivity values were approximately lower than 0.2 at lower strains in all deformation conditions. These m-values are typical of deformation controlled by dislocation glide or climb-limited glide processes characteristic of power-law creep [4]. The m-values at deformation temperatures of 850 and 900 °C

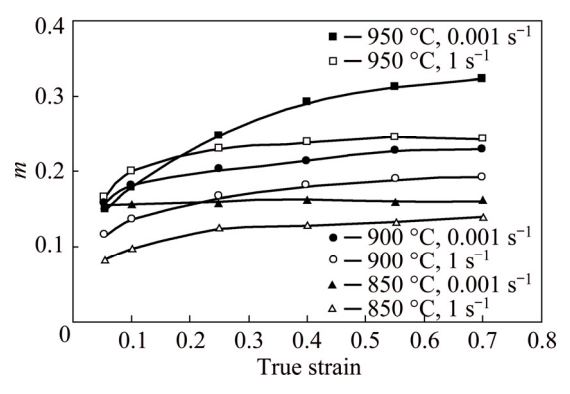
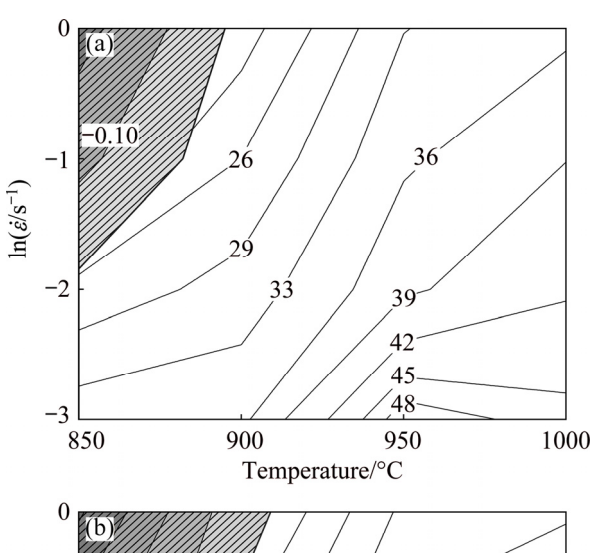


Fig. 11 Variation of strain-rate sensitivity of flow stress for Ti-6242S as function of strain at various deformation temperatures and strain rates

remained in power-law creep range (m<0.3) in all strain ranges; while the m-value increased to 0.33 with an increase in strain during deformation at 950 °C and $0.001 \,\mathrm{s}^{-1}$. Previous research [33] indicated that this was probably related to the dynamic globularization at high strains and also grain-boundary sliding (GBS). According to superplastic theory, the strain-rate sensitivity value is dependent on the alloy composition, grain size, volume fraction of phases and deformation parameters such as T, ε and $\dot{\varepsilon}$. Earlier studies on Ti-6Al-4V [34] and Ti60 [20] alloys have shown

that the maximum m-value was obtained at $0.93T_{\beta}$. The volume fractions of α and β phases are approximately equal at this temperature. Investigation [33] has shown that the 1:1 mixtures of these two phases can be contributed to the grain-boundary sliding. Now, by assuming that the β -transus temperature of the alloy in the present work is about 1010 °C, $0.93T_{\beta}$ will be equal to 939 °C, which is close to the deformation temperature of 950 °C. The microstructural observations also revealed that the volume fraction of α phase was approximately (47±2)% after deformation at 950 °C and 0.001 s⁻¹. Hence, hot deformation under these conditions leads to GBS and consequently has resulted in the maximum *m*-value.

Processing map at strain of 0.7 (Fig. 12(b)) exhibited a domain in the temperature range of 950-1000 °C and strain rate lower than 0.01 s^{-1} with a peak power dissipation efficiency of 55%.



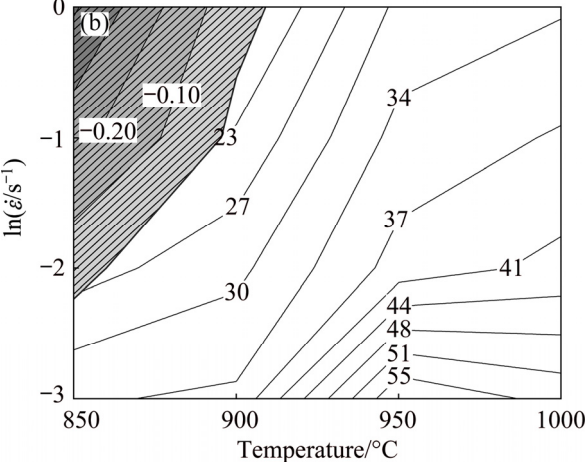


Fig. 12 Processing maps from hot compression data at strains of 0.4 (a) and 0.7 (b) (Numbers represent power dissipation efficiency (%); Shaded zone represents instability domain)

This value of power dissipation efficiency associated with strain-rate sensitivity higher than 0.3 may be attributed to superplasticity. JIA et al [20] claimed that some titanium alloys such as Ti60 exhibit superplasticity in this region.

3.3 Processing map of Ti-6242S alloy

In order to develop the processing map of the alloy, a dimensionless parameter called the efficiency of power dissipation, η , is defined as Eq. (1) [35]:

$$\eta(T,\dot{\varepsilon}) = \frac{2m}{m+1} \tag{1}$$

where m is the strain rate sensitivity of flow stress and given by $m = \partial \ln \sigma / \partial \ln \dot{\varepsilon}$. The power dissipation map is based on the variation of η with temperature and strain rate. The different domains in the power dissipation map are directly correlated with the specific microstructural mechanisms. In this map, the "safe" deformation conditions are dynamic recrystallization (DRX), dynamic recovery (DRV) and superplasticity, while flow localization and shear banding at high strain rates and wedge cracking are considered as "unsafe" deformation conditions. The spheroidization of lamellar structure occurs by the lamellae shearing and globularization, which is considered to be a type of DRX [18].

According to the microstructural changes, ZIEGLER [36] proposed the principles of maximum rate of entropy production, from which a condition for microstructural instability is obtained by Eq. (2):

$$\xi(\dot{\varepsilon}) = \frac{\partial \ln[m/(m+1)]}{\partial \ln \dot{\varepsilon}} + m \tag{2}$$

where $\xi(\dot{\varepsilon})$ is a dimensionless instability parameter. The dependence of dimensionless parameter on temperature and strain rate constitutes an "instability map". Flow instability is predicted to occur when $\xi(\dot{\varepsilon})$ becomes negative. This map should be superimposed onto the power dissipation map to obtain a processing map for the examined alloy. Figures 12(a, b) show the processing maps of the alloy which are obtained by superimposition of the efficiency of power dissipation map and the instability map at the true strains of 0.4 and 0.7, respectively. Clearly, η varies with the strain, temperature and strain rate. Generally, value of the efficiency increased with increasing strain and

temperature and decreasing the strain rate. Moreover, low efficiency regions coincided with the instability areas. Therefore, a reduction of efficiency at low temperature and high strain rate may be related to increasing the flow instability. By comparing the maps related to the true strain of 0.4 and 0.7, it was concluded that the degree of instability changes with strain as well. The instability area at the strain of 0.7 holds more negative ξ values, with the minimum of -0.4 under deformation condition of 850 °C and 1 s⁻¹, indicating that the deformation becomes more unstable as the strain increases. However, the value and expansion of instability region decreased with increasing the temperature, and an instability region at deformation temperature of 1000 °C and all strain rates could not be seen. One of the most important factors in reducing instability by increasing the temperature is the reduction of deformation heating effect as the main factor of an adiabatic shear banding. The previous study on Ti-6Al-4V alloy [37] has shown that, during hot deformation at 1030 °C, instability appears at strain rates higher than 10 s⁻¹ as well.

Processing map at strain of 0.7 showed an instability region at deformation temperature of 850 and 900 °C, and strain rates between 0.01 and 1 s⁻¹. The microstructures of the deformed specimens under various deformation conditions are shown in Fig. 13. Microstructural studies showed that the shear band formation is the dominant instability mechanism. As seen in Fig. 13(a), the microstructure exhibited large amount of band formed by a severe flow localization at about 45° with respect to the direction of compression. The flow localization is due to flow softening caused by the heat generated during deformation at high strain rates and low temperatures. As a result, the adiabatic heating is remained undissipated and made a considerable increase in temperature due to inadequate time interval [38]. Deformation heating calculation also showed that about temperature raise occurred during deformation at 850 °C and 0.1 s^{-1} .

Figure 13(b) shows the micrograph of the specimen deformed at 900 °C and 1 s⁻¹, where localized plastic flow can be observed at the center of compression specimen as a consequence of instability [13]. As seen, adjacent to this area, grains remained in their original form. This is undesirable



Fig. 13 Optical micrographs of specimens deformed under different conditions: (a) 850 °C, 0.1 s^{-1} ; (b) 900 °C, 1 s^{-1} ; (c) 1000 °C, 1 s^{-1}

in achieving appropriate mechanical properties and indicates that the deformation at low temperatures and high strain rates is dangerous and should be avoided. Similar results have been reported for other near- α titanium alloys [28].

The processing map of the alloy indicates that the deformation at temperatures above 950 °C and strain rate of 1 s⁻¹ was safe and flow instability was not observed. Micrograph of the deformed specimen at 1000 °C and $1 \, \mathrm{s}^{-1}$ is shown in

Fig. 13(c). No instability feature in mentioned deformation condition was found. It is worth noting that, despite the formation of shear bands at instability region ($T \le 900 \,^{\circ}\text{C}$, $\dot{\varepsilon} \ge 0.1 \,^{-1}$), there were no evidences of crack or cavity in the microstructures, nor in the macro-observation of the Ti-6242S alloy with acicular starting microstructure in all of the thermo-mechanical conditions. However, previous study by PRASAD et al [13] on the deformation behavior of the Ti-6242 alloy with thick-lamellar initial microstructure revealed that hot compression at 982 °C under the strain rate of 0.01 s⁻¹ led to creation of cavity at grain boundary triple junction. Besides, such behavior has been reported during deformation at strain rates higher than 1 s⁻¹ in the alloy with bimodal initial microstructure [39].

4 Conclusions

- (1) The flow stress behavior of the Ti-6242S alloy showed that high strains (~0.6) were necessary for reaching the steady state regime in temperature range of 850–950 °C, while at the deformation temperature of 1000 °C, steady state attained at lower strains (~0.1).
- (2) Deformation temperature played an important role in the microstructure features. The dynamic globularization occurred in the specimens deformed in lower part of two-phase α/β region ($T \le 950$ °C), and was intensified with an increase in the temperature and a decrease in the strain rate.
- (3) The deformation at 1000 °C elongated the β grains perpendicularly to the compression direction. Furthermore, β grain boundaries were serrated as a result of dynamic recovery and a few recrystallized grains were apparent in the vicinity of the deformed grain boundaries.
- (4) The developed processing map demonstrated that the deformation in the temperature range of 950–1000 °C and strain rates of 0.001–0.01 s⁻¹ was desirable and led to high efficiencies. On the other hand, increasing the strain rate and decreasing temperature led to an increase in flow instability, which was primarily manifested as adiabatic shear bands and local lamellae kinking.

References

- and texture evolution of a near- α titanium alloy during hot deformation [J]. Materials Science and Engineering A, 2013, 563: 16–20.
- [2] SHAMS S A A, MIRDAMADI S, ABBASI S M, KIM D, LEE C S. Mechanism of martensitic to equiaxed microstructure evolution during hot deformation of a near-alpha Ti alloy [J]. Metallurgical and Materials Transactions A, 2017, 48: 2979–2992.
- [3] LÜTJERING G, WILLIAMS J C. Titanium [M]. 2nd ed. Germany: Springer, 2007.
- [4] SEMIATIN S L, BIELER T R. The effect of alpha platelet thickness on plastic flow during hot working of TI-6Al-4V with a transformed microstructure [J]. Acta Materiallia, 2001, 49(17): 3565-3573.
- [5] AHMADIAN P, ABBASI S M, MORAKABATI M. The role of initial α-phase orientation on tensile and strain hardening behavior of Ti-6Al-4V alloy [J]. Materials Today Communications, 2017, 13: 332–345.
- [6] AHMADIAN P, ABBASI S M, MORAKABATI M. Effect of initial texture and grain size on geometrically necessary dislocations density distribution during uniaxial compression of Ti-6Al-4V [J]. Materials Today Communications, 2018, 14: 263-272.
- [7] SHELL E B, SEMIATIN S L. Effect of initial microstructure on plastic flow and dynamic globularization during hot working of Ti-6Al-4V [J]. Metallurgical and Materials Transactions A, 1999, 30: 3219–3229.
- [8] LI H, ZHAO Z L, GUO H Z, YAO Z K, NING Y Q, MIAO X P, GE M M. Effect of initial alpha lamellar thickness on deformation behavior of a near-α high-temperature alloy during thermomechanical processing [J]. Materials Science and Engineering A, 2017, 682: 345–353.
- [9] SEMIATIN S L, SEETERMAN V, WEISS I. Flow behavior and globularization kinetics during hot working of Ti-6Al-4V with a colony alpha microstructure [J]. Materials Science and Engineering A, 1999, 263: 257-271.
- [10] SEMIATIN S L, SEETERMAN V, WEISS I. The thermomechanical processing of alpha/beta titanium alloys [J]. JOM, 1997, 49(6): 33–39.
- [11] PARK C H, LEE B, SEMIATIN S L, LEE C S. Low-temperature superplasticity and coarsening behavior of Ti-6Al-2Sn-4Zr-2Mo-0.1Si [J]. Materials Science and Engineering A, 2010, 527: 5203-5211.
- [12] SEMIATIN S L, LAHOTI G D. Deformation and unstable flow in hot forging of Ti-6Ai-2Sn-4Zr-2Mo-0.1Si [J]. Metallurgical Transactions A, 1981, 12(10): 1705-1717.
- [13] PRASAD Y V R K, GEGEL H, DORAIVELU S M, MALAS J C, MORGAN T, LARK K A, BARKER D R. Modeling of dynamic material behavior in hot deformation: Forging of Ti-6242 [J]. Metallurgical Transactions A, 1984, 15(10): 1883–1892.
- [14] HAJARI A, MORAKABATI M, ABBASI S M, BADRI H. Constitutive modeling for high-temperature flow behavior of Ti-6242S alloy [J]. Materials Science and Engineering A,

- 2017, 681: 103-113.
- [15] EVANS R, SCHARNING P. Axisymmetric compression test and hot working properties of alloys [J]. Materials Science and Technology, 2001, 17(8): 995–1004.
- [16] DIETER G E, KUHN H A, SEMIATIN S L. Handbook of workability and process design [M]. USA: ASM International, 2003.
- [17] JIA W, ZENG W, LIU J, ZHOU Y, WANG Q. On the influence of processing parameters on microstructural evolution of a near alpha titanium alloy [J]. Materials Science and Engineering A, 2011, 530: 135–143.
- [18] LI A, HUANG L, MENG Q, GENG L, CUI X. Hot working of Ti–6Al–3Mo–2Zr–0.3Si alloy with lamellar $\alpha+\beta$ starting structure using processing map [J]. Materials and Design, 2009, 30(5): 1625–1631.
- [19] REZAEE M, ZAREI-HANZAKI A, MOHAMMADIZADEH A, GAHSEMI E. High-temperature flow characterization and microstructural evolution of Ti6242 alloy: Yield drop phenomenon [J]. Materials Science and Engineering A, 2016, 673: 346–354.
- [20] JIA Wei-ju, ZENG Wwi-dong, ZHOU Yi-gang, LIU Jia-rong, WANG Qing-jiang. High-temperature deformation behavior of Ti60 titanium alloy [J]. Materials Science and Engineering A, 2011, 528: 4068–4074.
- [21] MILLER R, BIELER T, SEMIATIN S. Flow softening during hot working of Ti-6Al-4V with a lamellar colony microstructure [J]. Scripta Materillia, 1999, 40(12): 1387–1393.
- [22] SONG H W, ZHANG S H, CHENG M. Dynamic globularization kinetics during hot working of a two phase titanium alloy with a colony alpha microstructure [J]. Journal of Alloys and Compounds, 2009, 480(2): 922–927.
- [23] ZHEREBTSOV S, MURZINOVA M, SLISHCHEV G, SEMIATIN S L. Spheroidization of the lamellar microstructure in Ti-6Al-4V alloy during warm deformation and annealing [J]. Acta Materillia, 2011, 59(10): 4138-4150.
- [24] WANJAR P, JAHAZI M, MONAJATI H, YUE S, IMMARIGEON J P. Hot working behavior of near-α alloy IMI834 [J]. Materials Science and Engineering A, 2005, 396: 50–60.
- [25] FLOWER H M. Microstructural development in relation to hot working of titanium alloys [J]. Materials Science and Technology, 1990, 6(11): 1082–1092.
- [26] HOSSENIN R, MORAKABATI M, ABBASI S M, HAJARI A. Development of a trimodal microstructure with superior combined strength, ductility and creep-rupture properties in a near alpha titanium alloy [J]. Materials Science and Engineering A, 2017, 696: 155–165.
- [27] GHAVAM M H, MORAKABATI M, ABBASI S M, BADRI H. Flow behavior modelling of IMI834 titanium alloy during

- hot tensile deformation [J]. Transactions of Nonferrous Metals Society of China, 2015, 25: 748–758.
- [28] HAN Yuan-fei, ZENG Wei-dong, QI Yun-lian, ZHAO Yong-qing. The influence of thermomechanical processing on microstructural evolution of Ti600 titanium alloy [J]. Materials Science and Engineering A, 2011, 528: 8410–8416.
- [29] STEFANSSON N, SEMIATIN S. Mechanisms of globularization of Ti-6Al-4V during static heat treatment [J]. Metallurgical and Materials Transactions A, 2003, 34(3): 691-698.
- [30] BUCKINGHAM R C, ARGYRAKIS C, HARDY M C, BIROSCA S. The effect of strain distribution on microstructural developments during forging in a newly developed nickel base superalloy [J]. Materials Science and Engineering A, 2016, 654: 317–328.
- [31] GOETZ R L, SEMIATIN S L. The adiabatic correction factor for deformation heating during the uniaxial compression test [J]. Journal of Materials Engineering and Performance, 2001, 10(6): 710–717.
- [32] KOIKE J, SHIMOYAMA Y, OHNUMA I, OKAMURA T, KAINUMA R, ISHIDA K, MARUYAMA K. Stress-induced phase transformation during superplastic deformation in two-phase Ti-Al-Fe alloy [J]. Acta Materiallia, 2000, 48(9): 2059-2069.
- [33] LUO Jiao, LI Miao-quan, YU Wei-xin, LI Hong. The variation of strain rate sensitivity exponent and strain hardening exponent in isothermal compression of Ti-6Al-4V alloy [J]. Materials and Design, 2010, 31(2): 741-748.
- [34] SASTRY S M L, LEDERISH R J, MACKY T L, KERR W R. Superplastic forming characterization of titanium alloys [J]. JOM, 1983, 35(1): 48–53.
- [35] MOHAMMADIZADEH A, ZAREI-HANZAKI A, ABEDI H R, MOTONEN S, PORTER D. Hot deformation characterization of duplex low-density steel through 3D processing map development [J] Materials Characterizations, 2015, 107: 293–301.
- [36] ZIEGLER H. Progress in solid mechanics [M]. New York: John Willey and Sons, 1963.
- [37] LUO J, LI M, YU W, LI H. Effect of the strain on processing maps of titanium alloys in isothermal compression [J]. Materials Science and Engineering A, 209, 504: 90–98.
- [38] MORAKABATI M, KHEIRANDISH S, ABOUTALEBI M, TAHERI A K, ABBASI S M. A study on the hot workability of wrought NiTi shape memory alloy [J]. Materials Science and Engineering A, 2011, 528: 5656–5663.
- [39] PRASAD Y V R K, SASIDHARA S. Hot working guide: A compendium of processing maps [M]. India, ASM International, 1997.

利用力学试验和热加工图分析近 α 钛合金的热加工行为

Maryam MORAKABATI, Alireza HAJARI

Faculty of Material & Manufacturing Technologies,

Malek-Ashtar University of Technology, Shabanlou Street, Tehran, Iran

摘 要:利用热加工图对具有针状初始组织的 Ti-5.7Al-2.1Sn-3.9Zr-2Mo-0.1Si (Ti-6242S)合金的热变形特征进行分析。单轴热压缩试验的温度为 850~1000 °C,应变速率为 $0.001\sim1~s^{-1}$ 。用热加工图确定合金的安全和不安全变形条件;利用扫描电镜(SEM)和光学显微镜(OM)分析合金的显微组织演变过程。研究发现,与在较低温度下变形相比,在 1000~°C 下变形后合金在流动软化行为中的流动应力存在差异,这是由于显微组织发生变化。在 950~°C 和 $0.001~s^{-1}$ 条件下变形,应变为 0.7的两相区加工图表现出较高的功率耗散效率,约为 55%,主要是由于发生大量球化。随着应变速率的增加和温度的降低,片层 α 相的球化减少,而扭折增加;最终,流动行为的失稳区发生在温度为 $850\sim900~°$ C、应变速率高于 $0.01~s^{-1}$ 的条件下,其主要机制为局部流动和绝热剪切。综合考虑功率耗散效率和显微组织,理想的变形条件为:变形温度 $950\sim1000~°$ C、应变速率 $0.001\sim0.01~s^{-1}$ 。该合金的最佳变形条件为:950~°C, $0.001~s^{-1}$ 。

关键词: Ti-6242S: 热变形: 加工图: 显微组织: 球化

(Edited by Bing YANG)